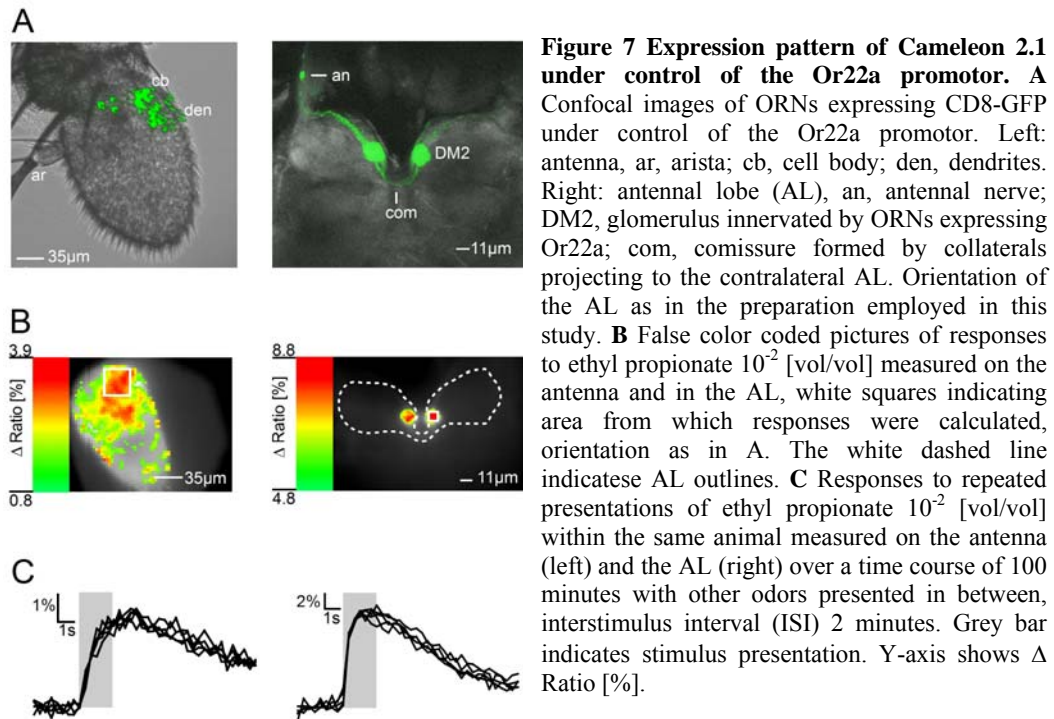


Results 1

Activity in ORNs expressing Or22a can be imaged on the antenna and within the AL

In order to characterize the molecular receptive range (MRR) of ORNs expressing Or22a we raised flies expressing the ratiometric Ca^{2+} sensor Cameleon2.1 (Fiala et al., 2002; Miyawaki et al., 1999) under control of the Or22a promoter (Vosshall et al., 2000). In the antennal preparation, expression of Cameleon2.1 in Or22a positive ORNs was visible through the intact cuticle as one or two large fluorescent areas in the dorsomedial position on the antenna, in agreement with the position published (Bhalerao et al., 2003; de Bruyne et al., 2001; Dobritsa et al., 2003) (Figure 7A left). Presentation of an odor which elicited a response (activating odor, see Materials and Methods) resulted in an increase in fluorescence intensity in the respective area (Figure 7B left). We did not observe any differences in our measurements when comparing the fluorescence changes in different stained areas on the same antenna. This observation suggests that ORNs expressing Or22a labeled in our flies form a homogenous population. Within a fly, repeated presentations of the same odor at the same concentration led to reproducible Ca^{2+} responses for up to 160 minutes (Figure 7C left).

In the AL preparation expression of Cameleon2.1 in Or22a ORNs could be seen in the antennal nerves, the glomeruli on both sides of the AL and in the commissure linking the left and right antennal lobe with each other (Figure 7A right). Presentation of an activating odor led to an identical increase in fluorescence activity within both glomeruli (Figure 7B right). If an antennal nerve was accidentally cut odor-evoked responses in the ipsilateral glomerulus were reduced in comparison to the contralateral glomerulus ($n = 4$ animals, data not shown). Just like on the antenna, within a fly the time course of a Ca^{2+} response to repeated presentations of the same odor at the same concentration was highly reproducible (Figure 7C right) for up to 100 minutes.



So far it has been assumed that the MRR of a glomerulus reflects the odor specificity of the OR expressed within the ORN innervating it (Friedrich and Korsching, 1997; Friedrich and Korsching, 1998; Wang et al., 2003). As a consequence the glomerular activity measured in the axon terminals of ORNs has been taken as representative of the OR MRR (Ng et al., 2002; Wang et al., 2003). However, it is possible that the initial MRR following sensory transduction in the ORN dendrites is changed within the glomerulus by the AL network before being transmitted to the next processing level, the antennal projection neurons (Aroniadou-Anderjaska et al., 2000; Ennis et al., 2001; Wachowiak et al., 2005; Wachowiak and Cohen, 1998; Wachowiak and Cohen, 1999). Hence we established the MRR in parallel on the antenna and within the AL.

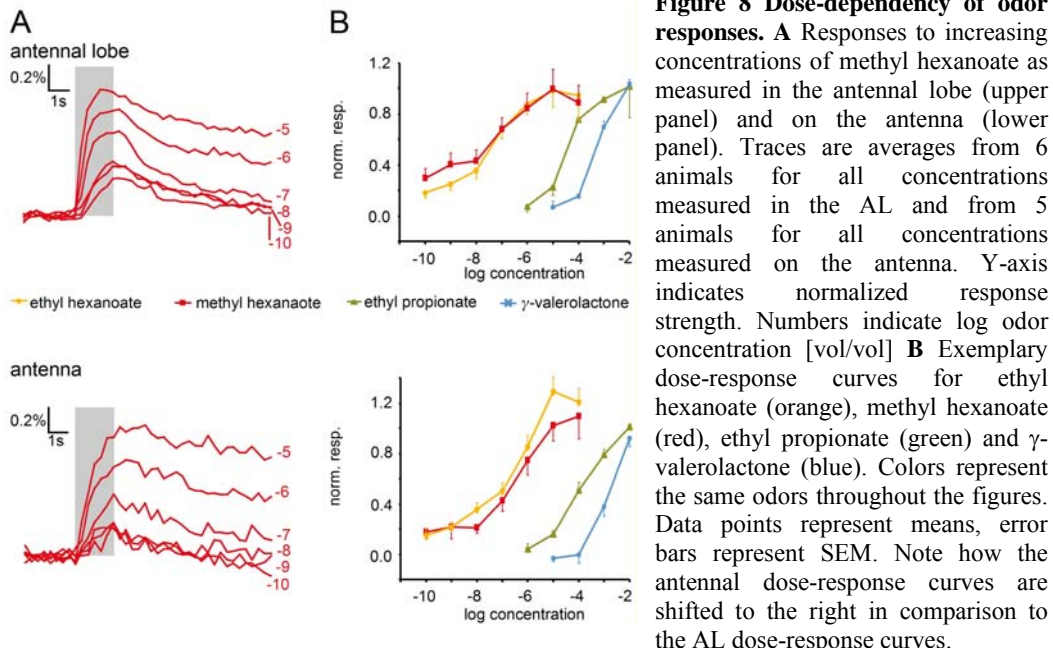
The characterization of an odor receptor's MRR can be regarded as a two-step process. The first step is to find an activating odor. This can be done by taking a 'shot gun' approach, i.e. screening the responses to a large number of odors from many different chemical classes in order to get a broad overview of the receptor's MRR (de Bruyne et al., 1999; de Bruyne et al., 2001; Zhao et al., 1998). The second step is taken

by systematically altering the structure of the most specific ligand found to define the MRR in more detail (Araneda et al., 2000; Spehr et al., 2003).

Accordingly, initially we tested the response to 104 odors from 9 different chemical classes (acids, alcohols, aldehydes, aromatics, ketones, N-rings, esters, O-rings, terpenes). The size of the molecules ranged from C3 to C20. We tested saturated and unsaturated straight chains, branched chains, cyclics and other chemical features (see Table 1 and 3, and Supplemental Table 1 and 2). In the first set of experiments we used a high concentration (10^{-2} [vol/vol]) in order not to mistake an activating odor for an inactivating odor because it was tested at a too low concentration. Out of the 104 substances tested 39 elicited a response which was clearly higher than those to the diluent (mineral oil) and a blank trial (air).

The MRR is identical for the antenna and the AL

The molecular receptive range of an ORN has two aspects: first, the chemical identity of the odors constituting it; second, the concentration range detected by the receptor for each odor, which is a measure for the odor's potency as a ligand. Therefore we tested the 39 activating odors at subsequently lower doses until no response was detectable any longer. As shown in Figures 8A, increasing the concentration of an activating odor lead to an increase of the response maximum until saturation was reached. To summarize the responses for further analysis we averaged three frames around the response maximum (see Materials and Methods). From these values we established dose-response curves for each activating odor. Figures 8B show four exemplary dose-response curves covering the odor concentrations eliciting responses in ORNs expressing Or22a. The colors represent the same odors throughout the figures.



From the 39 activating odors 10 reached saturation (defined as an increase in normalized response strength of less than 10% for a 10fold increase in concentration) at a concentration of 10^{-2} [vol/vol] or lower, with a dynamic range spanning between 3 and 4 log concentrations. In order to summarize the dose-response curves for each odor we fitted the Hill equation to the data (Meister and Bonhoeffer, 2001; Sachse and Galizia, 2003; Wachowiak and Cohen, 2001).

$$f(x) = a \times \frac{x^b}{(c^b + x^b)}$$

Where x stands for the odor concentration, $f(x)$ for the response elicited at concentration x , in this case the mean response across animals, a for the maximal response, b for the Hill coefficient which was estimated by the fit and represents a measure of the slope, and c for EC50, i.e. the Effective Concentration eliciting a half-maximal (i.e. 50%) response, also estimated from the fit.

For the EC50 to be a descriptor of an odor's specificity it needs to be representative for the ORN population (antenna) or the glomeruli (AL) rather than for the odor itself. Thus we defined the maximal response (a of the Hill equation) as the

overall maximal response measured in the AL or on the antenna. For the antenna the maximal response was elicited by 2-methyl butyl acetate at a concentration of 10^{-2} [vol/vol] (mean \pm SEM: 1.39 ± 0.05 , $n = 12$) and for the AL by ethyl 2-methyl butanoate at a concentration of 10^{-2} [vol/vol] (mean \pm SEM 1.31 ± 0.33 , $n = 3$). Note that the maximal response is not identical to the best ligand. As best ligand we defined the odor which needed the lowest concentration to elicit a halfmaximal response, i.e. the odor with the lowest EC50, as this odor was the most potent ligand for ORNs expressing Or22a.

The Hill coefficients of all dose-response curves were normally distributed (Kolmogorov-Smirnov normality test passed with $p = 0.115$ for AL and $p > 0.2$ for antennal dose-response curves). They were all below 1 (see Table 1) (mean_{AL} \pm SD: 0.532 ± 0.169 ; mean_{antenna} \pm SD: 0.501 ± 0.131) indicating independent interaction of individual odor molecules with the receptor. There was no significant difference between the antennal and the glomerular Hill coefficient (paired t-test, $t = 0.786$, $df = 48$, $p = 0.436$). Individual odors differed in the absolute range of concentrations at which they elicited responses. Ethyl hexanoate for example elicited responses at concentrations ranging from 10^{-9} [vol/vol] to 10^{-4} [vol/vol] whereas ethyl propionate elicited responses at concentrations ranging from 10^{-5} [vol/vol] to 10^{-2} [vol/vol] (Figure 8B). Figure 9A shows the MRR of ORNs expressing Or22a based on the EC50 estimated from fitting the Hill equation to the dose-response curves. We were able to estimate EC50 for all 39 activating odors identified in the initial screen for the AL data. However, for almost all odors a higher concentration was needed on the antenna than in the AL to elicit a response with comparable maximum (see Figure 8B). Thus, the antennal dose-response curves were systematically shifted to higher concentrations in comparison to the AL dose-response curves (Figure 8B). As a consequence we were only able to fit the Hill equation to the dose-response curves of 25 activating odors on the antenna. Figure 9B shows that the relationship between the antennal and the AL EC50 is linear ($EC50_{AL} = 1.0162 \times EC50_{ant} - 0.5786$; $R^2 = 0.9133$), indicating a strong correlation between them. For the remaining 14 activating odors we also found dose-dependent responses on the antenna although these odors elicited a response below the half-maximum at the highest concentration tested (10^{-2} [vol/vol]).

Table 1 Odors activating ORNs expressing Or22a.

	chemical name	CAS#	log EC50±SD (b) AL	log EC50±SD (b) ant	conformers ³
alcohol	1-butanol	71-36-3	-3.101±0.075 (0.556)	-2.402±0.042 (0.556)	8
	3-methyl-1-butanol	123-51-3	-2.921±0.057 (0.588)	-2.468±0.057 (0.639)	21
	1-hexanol	111-27-3	-2.648±0.097 (0.867)	-2.037±0.076 (0.726)	20
	E2-hexen-1-ol ¹	928-95-0	-2.307±0.056 (0.539)	0.498±0.083	24
	Z3-hexen-1-ol ¹	928-96-1	-1.966±0.068 (0.532)	0.489±0.112	na
	4-methylcyclohexanol ¹	25639-42-3	-2.145±0.112 (0.448)	0.329±0.096	5 (3)
	1-heptanol ¹	111-70-6	-2.289±0.096 (0.552)	0.261±0.008	35
	1-octen-3-ol	3391-86-4	-3.232±0.094 (0.692)	-2.419±0.065 (0.574)	37 (21)
3-octanol ¹	589-98-0	-2.799±0.059 (0.515)	0.406±0.113	71 (73)	
aldh.	pentanal ¹	110-62-3	-2.905±0.068 (0.486)	0.583±0.026	8
	hexanal ¹	66-25-1	-2.832±0.047 (0.399)	0.563±0.065	12
	heptanal	111-71-7	-4.81±0.026 (0.411)	-3.807±0.025 (0.393)	19
ester	ethyl acetate ¹	141-78-6	-2.015±0.031 (0.238)	0.475±0.052	3
	butyl acetate	123-86-4	-4.333±0.046 (0.583)	-3.343±0.032 (0.36)	12
	2-methyl butyl acetate	626-38-0	-4.886±0.051 (0.547)	-4.302±0.031 (0.478)	14 (10)
	pentyl acetate	628-63-7	-4.534±0.031 (0.519)	-4.125±0.019 (0.365)	20
	iso-amyl acetate	123-92-2	-4.163±0.025 (0.512)	-4.008±0.020 (0.388)	16
	hexyl acetate	142-92-7	-2.609±0.025 (0.331)	-2.736±0.042 (0.507)	39
	E2-hexenyl acetate	2497-18-9	-3.374±0.046 (0.594)	-3.220±0.035 (0.504)	11
	ethyl propionate	105-37-3	-4.174±0.036 (0.444)	-3.117±0.025 (0.423)	2
	propyl propionate ²	106-36-5	0.234±0.129		7
	ethyl butanoate	105-54-4	-5.872±0.02 (0.283)	-4.351±0.027 (0.437)	4
	ethyl (R)-(-)-3-hydroxybutanoate	24951-95-5	-3.334±0.069 (0.786)	-2.547±0.048 (0.597)	8
	ethyl (S)-(+)-3-hydroxybutanoate	56816-01-4	-2.842±0.116 (0.818)	-2.109±0.077 (0.524)	6
	ethyl 2-methylbutanoate	7452-79-1	-5.248±0.021 (0.313)	-4.33±0.047 (0.388)	7(10)
	butyl butanoate	109-21-7	-2.846±0.049 (0.419)	-2.858±0.045 (0.622)	4
	methyl pentanoate ²	624-24-8	0.647±0.056		17
	ethyl pentanoate ²	539-82-2	1.105±0.065		7
	methyl hexanoate	106-70-7	-6.898±0.034 (0.179)	-5.998±0.046 (0.316)	13
	methyl 3-hydroxy hexanoate	21188-58-9	-3.615±0.064 (0.751)		na
	ethyl hexanoate	123-66-0	-6.830±0.028 (0.248)	-6.615±0.034 (0.324)	15
	ethyl 3-hydroxyhexanoate	2305-25-1	-3.272±0.028 (0.591)	-2.429±0.054 (0.621)	8 (10)
propyl hexanoate ²	626-77-7	0.402±0.042		26	
methyl heptanoate ²	106-73-0	0.298±0.044		44	
ethyl heptanoate ²	106-30-9	0.304±0.027		44	
ketone	2-propanone ¹	67-64-1	-2.156±0.067 (0.58)	0.438±0.049	na
	2-butanone ¹	78-93-3	-3.085±0.07 (0.741)	0.596±0.067	2
	3-hydroxy-2-butanone ¹	513-86-0	-2.502±0.108 (0.548)	0.444±0.054	5 (5)
	2,3-butanedione ¹	431-03-8	-2.906±0.055 (0.433)	0.302±0.114	3
	3-penten-2-one	625-33-2	-3.502±0.04 (0.514)	-3.023±0.045 (0.504)	2
	2-hexanone ¹	591-78-6	-3.028±0.097 (0.704)	0.636±0.075	19
	3-hexanone	589-38-8	-3.121±0.068 (0.761)	-2.401±0.041 (0.404)	5
	cyclohexanone ¹	108-94-1	-2.405±0.123 (0.741)	0.397±0.053	2
2-heptanon	110-43-0	-3.084±0.038 (0.489)	-2.145±0.033 (0.379)	17	
O	β-butyrolactone	3068--88-0	-2.559±0.047 (0.563)	-2.155±0.061 (0.546)	1
	γ-valerolactone	108-29-2	-2.869±0.032 (0.773)	-2.381±0.148 (0.864)	1 (1)

CAS #, chemical abstract service number; b, Hill coefficient. Also see a complete list with all measured parameters in Supplemental Table 1; ¹ antennal responses did not reach a half-maximal response at 10⁻² [vol/vol], values given are mean ± SEM at 10⁻² [vol/vol]; ² only tested at a concentration of 10⁻⁵ [vol/vol] within the AL, values given are mean ± SEM; ³ number of conformers calculated for superpositioning of 3D molecules (Baum, 2005).

Table 2 Non-activating odors of ORNs expressing Or22a.

	chemical name	CAS#	chemical name	CAS#	
acid	propanoic acid	79-09-4	methyl propionate ¹	554-12-1	ester
	2-methyl propanoic acid	79-31-2	methyl butanoate ¹	623-42-7	
	butanoic acid	107-92-6	propyl butanoate ¹	105-66-8	
	3-methylbutanoic acid	503-74-2	hexyl butanoate	2639-63-6	
	pentanoic acid	109-52-4	propyl pentanoate ¹	141-06-0	
	heptanoic acid	111-14-8	butyl hexanoate ¹	626-82-4	
	nonanoic acid	112-05-0	nonanone	821-55-6	
alcohol	2,3-butanediol	513-85-9	indole	120-72-9	N
	cyclohexanol	108-93-0	furfural	98-01-1	O-ring
	octanol	111-87-5	acetyl furan	1192-62-7	
	decanol	112-30-1	γ -pentyl- γ -butyrolactone	104-61-0	
aldehyde	propanal	123-38-6	(R)-(-)-carvone	6485-40-1	terpene
	E2-hexenal	6728-26-3	(S)-(+)-carvone	2244-16-8	
	octanal	124-13-0	1,8-cineole	470-82-6	
	decanal	112-31-2	β -citronellol	106-22-9	
aromatic	phenylacetaldehyde	122-78-1	citral	5392-40-5	
	salicyl aldehyde	90-02-8	(S)-(-)-citronellal	106-23-0	
	2-hydroxy-anisole	90-05-1	(1R)-(-)-fenchone	7787-20-4	
	4-propenyl anisole	104-46-1	geraniol	106-24-1	
	benzaldehyde	100-52-7	geranyl acetate	105-87-3	
	4-methoxybenzaldehyde	123-11-5	(R)-(+)-limonene	5989-27-5	
	4-isopropylbenzaldehyde	122-03-2	linalool	78-70-6	
	4-methoxybenzene	100-66-3	(-)-menthone	14073-97-3	
	4-allyl-1,2-dimethoxybenzene	93-15-2	(1R)-(-)-myrtenal	564-94-3	
	2,4,5-trimethoxy-1-propenylbenzene (trans)	2883-98-9	(+)- α -pinene	7785-70-8	
	benzyl cyanide	140-29-4	(R)-(+)-pulegon	89-82-7	
	2-phenylethanol	60-12-8	α -terpineole	10482-56-1	
	phenylethanone	98-86-2	(-)- α -thujone	546-80-5	
	eugenol	97-53-0	α -bisabolol	515-69-5	
	iso-eugenol	97-54-1	β -caryophyllene	87-44-5	
	4-methylphenol	106-44-5	E,E-farnesol	106-28-5	
	4-ethylphenol	123-07-9	heptane	142-82-5	other
	2-propylphenol	644-35-9	octane	111-65-9	
	3-phenyl-2E-propenal	14371-10-9	nonane	111-84-2	
	methylsalicylate	119-36-8	Z11-hexadecenyl acetate	34010-21-4	
octyl acetate	112-14-1	Z11-octadecenyl acetate	1775-43-5		
decyl acetate	112-17-4				

CAS #, chemical abstract service number; k, ketone; N, N-ring; ¹ odor was only tested at a concentration of 10⁻⁶[vol/vol]; ² odor elicited a small response at 10⁻²[vol/vol]; ³ inactivating odour. Also see Supplemental Table 2 for measured parameters.

Two odors of the MRR were clearly distinct from the remaining ones: ethyl and methyl hexanoate needed by far the lowest concentration to elicit a halfmaximal response (mean log EC50 \pm SD AL/antenna: ethyl hexanoate = -6.83 \pm 0.028 / -6.615 \pm 0.034; methyl hexanoate = - 6.898 \pm 0.034 / -5.998 \pm 0.046). These odors had an

EC50 more than 10 times lower than the next best odor ethyl butanoate (mean log EC50 \pm SD AL/antennae: ethyl butanoate = -5.872 ± 0.020 / -4.351 ± 0.027 ; see Figure 9A and B and Table 1).

These results show that the same odors belong to the antennal and the AL MRR (for molecular structure of odors activating Or22a see Figure 10). Concerning the concentration ranges at which each odor elicited a response, we found a systematic shift between the antennal and the AL MRRs. Because of the shift being systematic the relative concentration ranges at which the odors elicited a response were identical for the antennal and the AL MRR. Furthermore, the same odors were identified as most potent ligands for both MRRs. Thus, we conclude that antenna and AL have the same molecular receptive range.

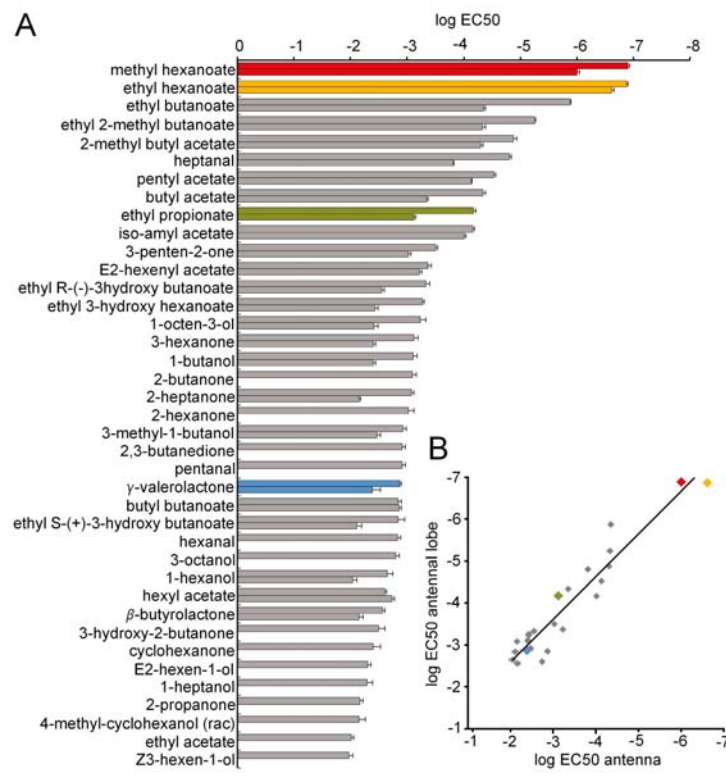


Figure 9 Molecular receptive range of ORNs expressing Or22a. **A** EC50 values were estimated based on Hill equations fitted to individual dose-response curves with a non-linear least-squares algorithm. Upper bars show the EC50 based on AL measurements, lower bars show the EC50 based on antennal measurements. Error bars indicate standard deviation. Color code is identical to Figure 8. Odors are sorted from lowest EC50 to highest. **B** Correlation between 25 odors for which the EC50 could be estimated both on the antenna and within the AL. The correlation equation was $EC50_{AL} = 1.0162 \times EC50_{ant} - 0.5786$ $R^2 = 0.9133$

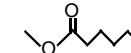
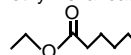
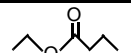

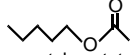
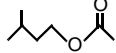
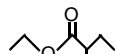
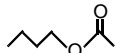
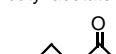
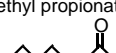
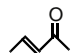

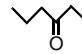
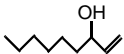
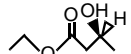
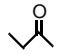
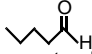
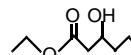
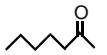
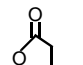
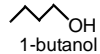
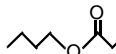

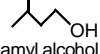
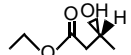
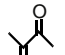
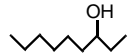
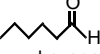
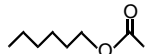
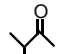
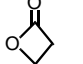
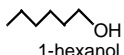





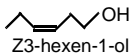
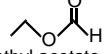
alcohols	aldehydes	esters	ketones	O-rings	EC50
		 methyl hexanoate			10^{-7}
		 ethyl hexanoate			10^{-6}
		 ethyl butanoate			10^{-5}
	 heptanal	 pentyl acetate			10^{-5}
		 2-methyl butyl acetate			10^{-5}
		 ethyl 2-methyl-butanoate			10^{-4}
		 butyl acetate			10^{-4}
		 ethyl propionate			10^{-4}
		 iso-amyl acetate	 3-penten-2-one		10^{-3}
		 E2-hexenyl acetate	 3-hexanone		10^{-3}
 1-octen-3-ol		 ethyl (R)-(3)-hydroxy-butanoate	 2-butanone		10^{-3}
	 pentanal	 ethyl 3-hydroxy hexanoate	 2-heptanone	 γ -valerolactone	10^{-3}
 1-butanol		 butyl butanoate	 2-hexanone		10^{-3}
 iso-amyl alcohol		 ethyl (S)-(3)-hydroxy-butanoate	 2,3-butanedione		10^{-3}
 3-octanol	 hexanal	 hexyl acetate	 3-hydroxy-2-butanone	 β -butyrolactone	10^{-3}
 1-hexanol					10^{-2}
 E2-hexen-1-ol			 cyclohexanone		10^{-2}
 1-heptanol			 2-propanone		10^{-2}
 4-methyl-cyclohexanol					10^{-2}
 Z3-hexen-1-ol		 ethyl acetate			10^{-2}

Figure 10 Chemical structures of odors belonging to the Or22a MRR. Across columns odors are sorted according to their chemical class. Within columns odors are sorted according to their EC50 (indicated to the right).

Dynamics of the Ca²⁺ responses show differences between antenna and AL

Electrophysiological studies have shown that besides the response amplitude being odor and concentration specific so are also the temporal dynamics of the odor-evoked response (de Bruyne et al., 2001). The same was found for the odor-evoked Ca²⁺ responses. We evaluated several parameters: time of response onset, time of maximum, rise time (defined as time elapsing between the time point of 10% and 90% of maximum), response maximum, fall time (defined as time elapsing between the time point of 90% and 66% of maximum) and response duration (defined as time elapsing between the time point of 10% of the maximum before the maximum and the time point of 66% of the maximum after the maximum) (Figure 11A). Each odor elicited a concentration dependent time course of the Ca²⁺ response which was reproducible across animals. For a given odor the response parameters changed with increasing odor concentration (Figure 11B). The rise time changed differently between antennal and AL responses with increasing odor concentration. Within the AL the rise time decreased with increasing odor concentrations and the response maximum was reached earlier. For the antenna however, the rise time increased with increasing odor concentrations and the maximum of the response occurred successively later. Response maximum, fall time and response duration on the other hand both increased with increasing odor concentration for antennal as well as for AL responses.

In order to compare responses with the same maximum in the AL, in the antenna and between both we calculated putative EC50 time traces. These traces were estimated based on the time trace elicited by the concentration below and above the actual EC50. Figure 11C and 11D show representative traces of the most distinct response types. The first response type was characterized by a short rise and fall time (e.g. ethyl propionate). The second response type had a short rise time and a longer fall time than the first response type (e.g. methyl hexanoate). The third response type was characterized by a late response onset, an elongated rise and fall time in comparison to the two other response types (e.g. γ -valerolactone). Figure 11C shows the different response types in the AL and on the antenna. At first sight the antennal and AL response types are very similar to each other. However, comparing the antennal response types to the respective AL response types in more detail (Figure

11D) revealed that antennal responses had a longer rise time (AL = 1.042s, antenna = 1.405s, Wilcoxon signed rank test for all following comparisons of response parameters, $p \leq 0.001$). The longer rise times on the antenna were due to a delayed time of response maximum (AL = 3.794s, antenna = 4.327s, $p \leq 0.001$) as well as to an earlier response onset (AL = 2.746s, antenna = 2.908s, $p \leq 0.001$). Furthermore, antennal responses showed longer fall times (AL = 1.321, antenna = 1.818, $p \leq 0.001$).

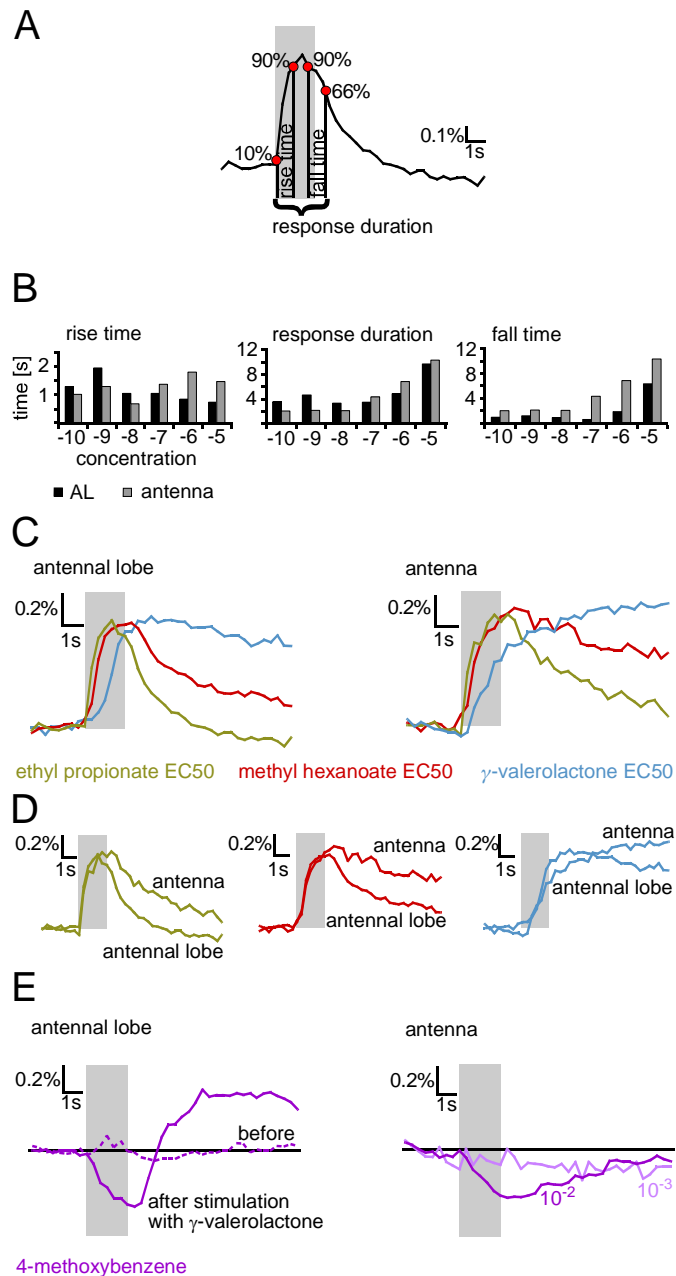


Figure 11 Time course of Ca^{2+} responses is odor and concentration dependent. **A** Exemplary time course of a calcium response upon presentation of an activating odor indicating how response parameters were defined. Y-axis indicates normalized response strength. Response onset was defined as time of 10% of the response maximum. Rise time was defined as time elapsing between 10% and 90% before the response maximum. Fall time was defined as time elapsing between 90% and 66% after the response maximum. Response duration was defined as time elapsing between 10% before the response maximum and 66% after the response maximum. **B** Shown are rise time, response duration, and fall time both for AL (black) and antennal (grey) measurements to increasing concentrations of methyl hexanoate. Note how AL and antennal rise times change differently across concentrations but response duration and fall time change similarly. Y-axis indicates time in seconds, x-axis indicates log concentration. **C** Putative responses at EC50 of ethyl propionate (green), methyl hexanoate (red) and γ -valerolactone (blue) for the antennal lobe (left panel) and the antenna (right panel). Responses were calculated based on the response measured to the concentration below and above EC50. Each of the traces is representative of a distinct response type, ethyl propionate = type I, methyl hexanoate = type II, γ -valerolactone = type III. Y-axis indicates normalized response strength. **D** Comparison of the response types between antennal lobe and antenna. Color code as in C. Note how the rise time of the antennal responses is always longer in comparison to the AL responses due to the response maximum being reached later. Also note the longer fall time of the antennal responses in comparison to the AL responses. **E** Inactivating odors. Y-axis shows normalized response strength. Right panel shows averaged antennal responses to 4-methoxybenzene at a concentration of 10^{-2} [vol/vol] ($n = 4$) and 10^{-3} [vol/vol] ($n = 9$). Left panel shows averaged AL responses to presentation of 4-methoxybenzene at a concentration of 10^{-2} [vol/vol] before ($n = 8$) and after ($n = 5$) presentation of γ -valerolactone 10^{-2} [vol/vol].

Another difference in the Ca^{2+} dynamics between antenna and AL was observed for inactivating odors. As shown in Figure 11E stimulation with 4-methoxybenzene at a concentration of 10^{-2} [vol/vol] evoked a decrease in fluorescence intensity on the antenna, while a lower concentration (10^{-3} [vol/vol]) did not evoke a response. In the AL however, 4-methoxybenzene (10^{-2} [vol/vol]) did not elicit a response under standard conditions. Surprisingly, a decrease in fluorescence intensity was visible when 4-methoxybenzene (10^{-2} [vol/vol]) was presented after presentation of an odor with a long-lasting response, e.g. γ -valerolactone at a concentration of 10^{-2} [vol/vol]. We observed the same phenomenon for benzaldehyde (data not shown). It is known from previous studies that ORNs expressing Or22a have a low spontaneous firing frequency (4Hz) (de Bruyne et al., 2001; Dobritsa et al., 2003; Hallem et al., 2004). Under standard conditions 4-methoxybenzene (10^{-2} [vol/vol]) might decrease the spiking frequency from 4 to at most 0 Hz. Thus, the data presented in Figure 11E indicate that the resulting change in Ca^{2+} concentration might be too small to be detected by Cameleon2.1. Presentation of a long-lasting stimulus elevated the Ca^{2+} concentration (data not shown) by presumably raising the spontaneous ORN firing frequency. Due to the elevated Ca^{2+} concentration presentation of 4-methoxybenzene (10^{-2} [vol/vol]) might have led to a larger decrease in Ca^{2+} concentration which then

was detectable by Cameleon2.1. The results also indicate that the overall magnitude of the Ca^{2+} decrease is larger in the antenna at resting Ca^{2+} levels than in the AL.

Influence of inhibitory AL network

In order to test whether the longer antennal responses were cut off via presynaptic inhibition by the AL network the ionotropic GABA receptor agonist muscimol and the Cl^- channel blocker picrotoxin (PTX) were applied to the AL. Both PTX and muscimol have been shown to be effective in the *Drosophila* olfactory system (Rosay et al., 2001; Wilson et al., 2004; Wilson and Laurent, 2005). The odors tested varied both in their EC_{50} , i.e. in their potency as ligands for Or22a, and in their response type. Ethyl hexanoate, which elicits a type 2 response, and 1-butanol, which elicits a type 1 response, were chosen. Ethyl hexanoate, the best ligand identified, was tested at a concentration of 10^{-7} [vol/vol] (log EC_{50} -6.83) and 1-butanol was tested at a concentration of 10^{-3} [vol/vol] (log EC_{50} -3.101). As we were interested in the input to the AL network we also looked at the response pattern elicited by these odors across the entire ORN population. To this end the odor responses in flies expressing Cameleon2.1 under control of the Or83b promoter, which is expressed in 70% to 80% of the antennal ORNs (Larsson et al., 2004), were recorded. Ethyl hexanoate 10^{-7} [vol/vol] only elicited a response in two dorso-medial glomeruli which were tentatively identified as DM2 based on their position within the AL and their physiological response (Figure 12A). 1-butanol 10^{-3} [vol/vol] on the other hand elicited a broad pattern across many glomeruli (Figure 12A).

Muscimol applied at a concentration of $500\mu\text{M}$ significantly reduced the responses to both odors in ORNs expressing Or22a (5 of 5 flies, paired t-test, $p = 0.025$ for 1-butanol, $p = 0.045$ for ethyl hexanoate, Figure 12B). Interestingly, the response to ethyl hexanoate was slightly more reduced than that to 1-butanol (4 of 5 flies, mean ((response after muscimol/response before muscimol) $\times 100$) \pm SEM: 1-butanol = $55\% \pm 11.6\%$, ethyl hexanoate = $43\% \pm 14.8\%$, paired t-test $p = 0.08$). The effect was partly washable (Figure 12C, compare dashed line to grey line). Furthermore, it was found that the resting Ca^{2+} level was reduced after application of

muscimol and returned slightly to control levels after the wash (Figure 12D, compare to reduction of Ca^{2+} level with PTX and the Ringer control). This finding is in agreement with a model where spontaneous ORN action potentials lead to a certain Ca^{2+} resting level. Application of muscimol could result in activation of ionotropic GABA receptors on the ORN presynaptic terminals leading to hyperpolarization. This hyperpolarization would prevent spontaneous ORN action potentials thereby reducing the resting Ca^{2+} level. Thus, these results provide evidence for presynaptic inhibition of ORN responses.

PTX applied at a concentration of $5\mu\text{M}$ elicited a significant increase in the response to 1-butanol (4 of 8 flies, paired t-test, $p = 0.023$, Figure 12B). The increased response to 1-butanol was due to an increase in response amplitude and not to an increase in response duration (Figure 12C). Interestingly, PTX application did not change the response to ethyl hexanoate (paired t-test, $p = 0.555$, $n = 8$, Figure 12B). From these results we conclude that the differences in antennal and AL response dynamics are not due to presynaptic inhibition. Furthermore, the presynaptic inhibition of ORNs was odor-specific.

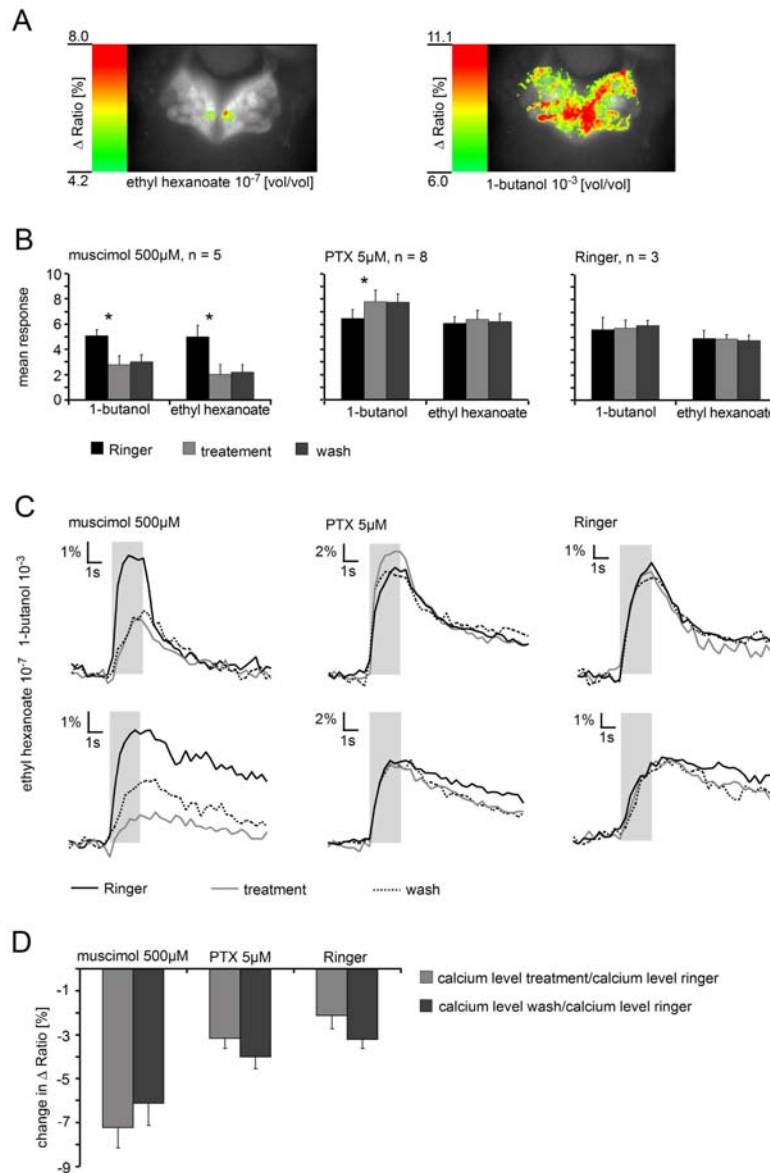


Figure 12 Presynaptic inhibition of ORNs expressing Or22a. **A** Responses to ethyl hexanoate (10^{-7} [vol/vol]) and to 1-butanol (10^{-3} [vol/vol]) measured in flies expressing Cameleon 2.1 under control of the Or83b promoter. Note how ethyl hexanoate only evokes a response in one glomerulus whereas 1-butanol evokes responses in several glomeruli. **B** Influence of muscimol (500 μ M) and picrotoxin (PTX) (5 μ M) on odor-evoked responses in ORNs expressing Or22a and innervating DM2. Values represent averages of mean responses to presentations of 1-butanol (10^{-3} [vol/vol]) and ethyl hexanoate (10^{-7} [vol/vol]) with Ringer, pharmacon and after wash. Error bars indicate SEM of mean responses. Application of muscimol resulted in decreased responses to both odors (paired t-test before vs after application of muscimol: $p = 0.025$ for 1-butanol, $p = 0.045$ for ethyl hexanoate), whereas application of PTX resulted only in an increase of the response to 1-butanol (10^{-3} [vol/vol]) (paired t-test before vs after application of PTX: $p = 0.023$ for 1-butanol, $p = 0.555$ for ethyl hexanoate). **C** Influence of muscimol and PTX on time courses of odor-evoked Ca^{2+} responses. Upper row shows responses to 1-butanol 10^{-3} [vol/vol], lower row shows responses to ethyl hexanoate 10^{-7} [vol/vol]. Traces show single animals. Note the different scaling of the y-axis. **D** Influence of muscimol and PTX on resting Ca^{2+} levels. Graphs show percentage change in prestimulus D Ratio [%] representative of the overall Ca^{2+} resting level after application of pharmacon and after wash of pharmacon in comparison to resting Ca^{2+} levels before pharmacon application. Graphs show mean \pm SEM, $n = 5$ for muscimol, $n = 8$ for PTX, $n = 3$ for Ringer.

Temporal response parameters depend on the chemistry of the odors

We were interested in finding a systematic relationship between the odors and the response types elicited by them. The odors representing the response types in Figure 11C and 11D differed in their EC50 (see Figure 9 and Table 1). Thus a correlation between an odor's EC50 and the time course elicited by it seemed possible. By sorting the different response parameters according to the respective odor's EC50 we were not able to find such a correlation neither for the AL (Figure 13) nor for the antenna (data not shown but see Supplemental Table 1).

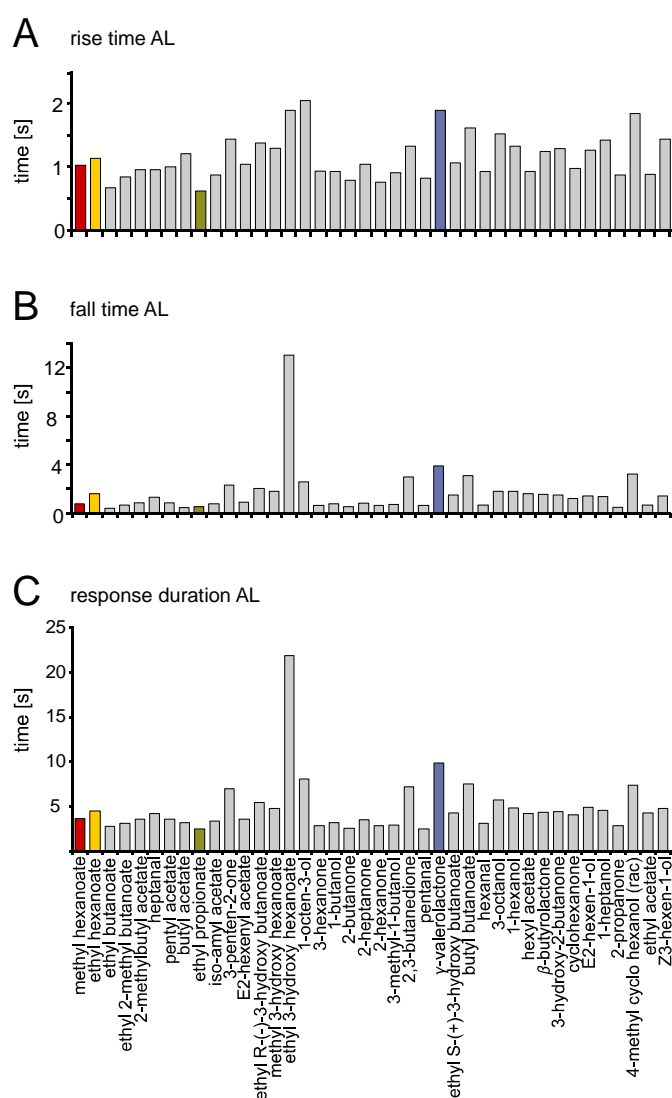


Figure 13 Response parameters for all odors of the molecular receptive range at EC50. Color code as in all previous figures. Odors are sorted by increasing EC50 from left to right. **A** Rise time. **B** Fall time. **C** Response duration. For definition see figure 11A. Y-axis indicates seconds. Note that there is no obvious relationship between EC50 and either of the parameters.

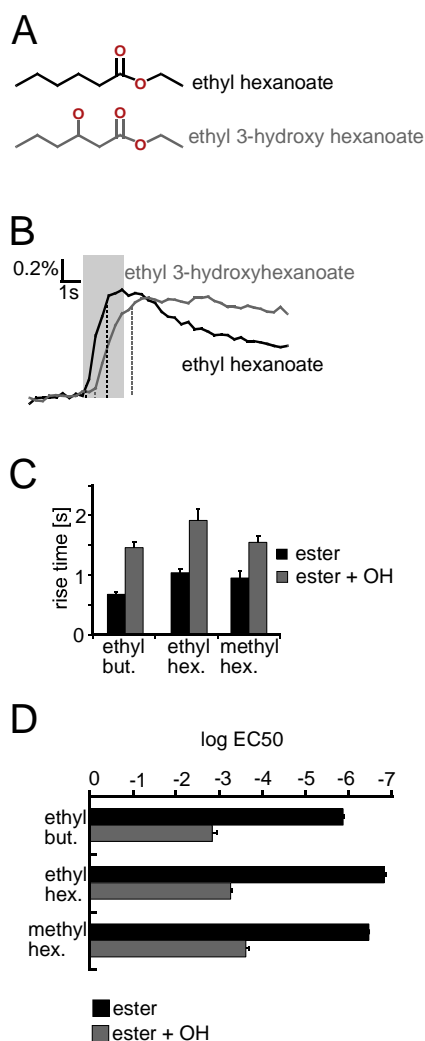


Figure 14 Relationship between chemistry of an odor and its response dynamics. **A** Chemical structure of an ester ‘pair’. Black indicates the ester ethyl hexanoate. Grey indicates the same odor with an additional hydroxyl group at the third carbon atom of the carboxylic acid moiety of the ester, namely ethyl 3-hydroxy hexanoate. **B** Responses to ethyl hexanoate at a concentration of 10^{-6} [vol/vol] (black) and to ethyl 3-hydroxy hexanoate at a concentration of 10^{-3} [vol/vol] (grey). Traces indicate mean ($n = 8$ for ethyl hexanoate, $n = 9$ for ethyl 3-hydroxy hexanoate). Dashed lines indicate 10% and 90% of response maximum, i.e. show rise time (Figure 11A). Grey vertical bar represents odor presentation. Note that the maxima of the responses are almost identical but how the rise time of the response to ethyl 3-hydroxy hexanoate is elongated in comparison to that of ethyl hexanoate. **C** Three ester pairs were tested where the additional hydroxyl group led to an increase in the rise time of the response. For the analysis responses of comparable amplitudes (normalized response strength) were chosen (mean max \pm SEM: ethyl hexanoate = 0.92 ± 0.1 , ethyl 3-hydroxy hexanoate = 0.91 ± 0.05 , methyl hexanoate 10^{-5} = 0.95 ± 0.11 , $n = 6$, methyl 3-hydroxy hexanoate 10^{-3} = 1.04 ± 0.06 , $n = 8$, ethyl butanoate 10^{-4} = 1.14 ± 0.05 , $n = 9$, ethyl 3-(S)-(+)-hydroxy hexanoate 10^{-2} = 1.08 ± 0.1 , $n = 10$; One-way ANOVA $F = 1.334$, $p = 0.268$). In all cases the response to the odor with the additional hydroxyl group at the 3rd carbon atom of the carboxylic acid moiety had a significantly longer rise time than the straight chain ester (ethyl hexanoate = $1.038s \pm 0.0699$, ethyl 3-hydroxy hexanoate = $1.917s \pm 0.185$, $p = 0.002$; methyl 3-hydroxy hexanoate = $0.951s \pm 0.107$, methyl 3-hydroxy-hexanoate = $1.549s \pm 0.111$, $p = 0.008$; ethyl butanoate = $0.674s \pm 0.0460$, ethyl 3-(S)-(+)-hydroxy-hexanoate = $1.459s \pm 0.09$, $p \leq 0.001$). **D** Esters with an additional hydroxyl group had a higher EC50 than the respective esters without the hydroxyl group. Log EC50 \pm SD: ethyl butanoate = -5.872 ± 0.02 ; ethyl S-(+)-hydroxy butanoate = -3.334 ± 0.069 ; ethyl hexanoate = -6.83 ± 0.028 , ethyl 3-hydroxy hexanoate = -3.272 ± 0.028 ; methyl hexanoate = -6.462 ± 0.027 , methyl 3-hydroxy hexanoate = -3.615 ± 0.064 .

Instead, we found a correlation between the response parameters and the chemistry of a group of esters. As shown in Figure 14 an additional hydroxyl group at the 3rd carbon atom of the carboxyl acid moiety (Figure 14A) fundamentally changed the time course of the Ca^{2+} response. Given the same response amplitude, responses to the esters without an additional hydroxyl group had a significantly shorter rise time than esters with an additional hydroxyl group at the third carbon atom of the carboxylic acid moiety, both on the antenna and in the AL (Figures 14B and 14C, antennal data not shown). Additionally, esters without the additional hydroxyl group

had a lower EC50 value than those with the additional hydroxyl group. This was found to be true for ethyl and methyl hexanoate as well as for ethyl butanoate, the odors for which we tested the respective hydroxylated / unhydroxylated pairs (Figure 14D).

These results show that the chemistry of an odor directly influences the temporal pattern of the response elicited by it. Therefore it is most likely that the differences in the response dynamics of individual odors is related to the interaction between the odor molecule and the receptor it interacts with.

Which odor properties are responsible for activating Or22a?

We used saturated vapor as odor stimuli. Vapor pressure however varies for different chemicals. Therefore, although the absolute volume of each odor for a given concentration was the same, the number of molecules presented to the flies at a given concentration differed for individual odors. Thus differences in response strength for different odors at a given concentration could simply result from differences in the number of ppm reaching the antenna. It would be possible that odors with a lower EC50 only seem to be better ligands because of the higher number of molecules reaching the antenna at low vol/vol concentrations. Cometto-Muniz and co-workers (2003) described the relationship between liquid- and vapor-phase concentrations for 60 volatile organic compounds diluted in mineral oil. From this equation and the vapor pressures available for odors activating Or22a we were able to estimate the ppm at EC50 for 23 odors (see Materials and Methods and Supplemental Table1). If Or22a was purely activated by the number of molecules reaching it all odors would need the same number of ppm to elicit a halfmaximal response. Thus at EC50 all odors should have the same number of ppm. However, as shown in Figure 15, odors needing a low vol/vol concentration to elicit a halfmaximal response also need a low number of ppm to elicit a half-maximal response. Hence we conclude that it is not the number of molecules reaching Or22a which is responsible for the response strength elicited by an individual odor at a given concentration. Therefore, we subsequently examined the chemistry of the activating odors in more detail.

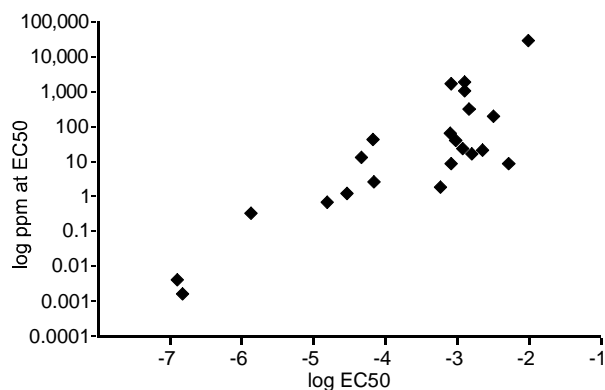


Figure 15 Number of ppm at EC50.

The graph shows the log number of ppm at EC50 plotted against the log EC50 concentration for 23 odors where estimation of ppm based on vapor pressure was possible. Odors that need a low concentration to elicit a halfmaximal response also needed a low number of ppm to elicit a halfmaximal response.

Or22a odotopes

The parts of an odor molecule putatively responsible for the interaction of this odor with a particular receptor have been termed odotopes (Mori and Shepherd, 1994). In order to find possible odotopes common to the odors included in the MRR of Or22a we compared an odor's chemistry and its EC50. An odor's EC50 was considered to be a measure of its potency as ligand for Or22a. Or22a has a broad response spectrum as we found graded responses to 39 out of 104 odors tested (Figure 9). Nonetheless ORNs expressing Or22a are not responding arbitrarily to all odors presented. Among the 10 odors with the lowest EC50 are 9 esters. All of these range from C8 to C5. Heptanal as an aldehyde is the only non-ester among the best ligands. Odors from other chemical classes only elicited responses at far higher concentrations (first ketone to elicit a response was 3-penten-2-one with a log EC50 of -3.502; first alcohol eliciting a response was 1-octen-3-ol with a log EC50 of -3.232; second aldehyde after heptanal: pentanal with a log EC50 of -2.905, Figure 9A).

Among the 104 odors tested there were several classes of non-activating odors: none of the aromates, terpenes or acids tested elicited a response (Table 2 and Supplemental Table 2). An exception was propionic acid which elicited a small response at a concentration of 10^{-2} [vol/vol]. There were some rules distinguishing non-activating from activating odors. Although we found very good responses to most of the esters tested, there were several which did not elicit a response at all (octyl acetate, decyl acetate, hexyl butanoate). These had in common that they were all larger than the activating odors. Additionally, we observed that smaller esters needed

higher concentrations to elicit a halfmaximal response. Furthermore, the length of the alcohol and the carboxylic acid moiety forming the ester seemed to play a crucial role: the esters ethyl hexanoate and hexyl acetate have the same molecular formula ($C_8H_{16}O_2$) but ethyl hexanoate has a very low EC50 ($\log EC50 = -6.83$) whereas hexyl acetate has an approximately 16,000 times higher EC50 ($\log EC50 -2.609$). The molecules differ from each other in that ethyl hexanoate is the product of a C2 alcohol and a C6 carboxylic acid whereas hexyl acetate is the product of a C6 alcohol and a C2 carboxylic acid. However, the results from the initial ‘shotgun’ approach were not detailed enough to pin these observations down to common odotopes. In order to find such common odotopes we tested odors whose molecular structure varied systematically from those of the best ligands, namely ethyl and methyl hexanoate.

For this experiment we only tested the odors at a single concentration. We chose 10^{-6} [vol/vol], the concentration at which both ethyl and methyl hexanoate elicit responses which are at the upper end of their dose-response curve (Figure 8B). The odors we picked varied both in the length of the alcohol moiety (ranging from CI - methyl to CIV - butyl) and in the length of the carboxylic acid moiety (ranging from C3 - propionate to C7 - heptanoate), i.e. at both sides of the ester group (Figure 16). We confirmed that ethyl and methyl hexanoate are the best ligands for ORNs expressing Or22a. We also confirmed the general size limit for esters: all C9 and C10 odors tested (propyl hexanoate, butyl hexanoate, ethyl heptanoate) only elicited rather small responses, just above the noise level. Additionally, all esters below C6 (methyl propionate, ethyl propionate, methyl butanoate) did not elicit a response. We also confirmed a size limit at both sides of the ester bond. For the alcohol moiety we found that whereas methyl and ethyl hexanoate both elicited a large responses (CI and CII, mean \pm SEM: 1.279 ± 0.05 , 1.274 ± 0.03) propyl hexanoate only elicited a very small response (CIII, mean \pm SEM: 0.402 ± 0.04) and butyl hexanoate did not elicit a response at all (CIV, mean \pm SEM: 0.111 ± 0.02). Additionally, none of the propyl esters elicited a large response (mean \pm SEM: propyl pentanoate 0.069 ± 0.03 , propyl butanoate 0.106 ± 0.03 , propyl propionate 0.234 ± 0.05). Thus we conclude that propyl, i.e. C3 alcohol moieties, are too long. For the ethyl (CII) and methyl (CI) moiety there was no difference among the hexanoates. However, looking at the pentanoates (C5) and the butanoates (C4) it became obvious that the ethyl moiety seemed to be more effective at eliciting a response than the methyl moiety.

Concerning the carboxylic acid moiety we observed that increasing the chain length had a stronger effect than decreasing the chain length: methyl and ethyl heptanoate (C7) elicited much smaller responses (mean \pm SEM: 0.298 ± 0.04 , 0.304 ± 0.03) than did methyl and ethyl pentanoate (C5, mean \pm SEM: 0.647 ± 0.06 , 1.105 ± 0.06) in relation to the responses elicited by methyl and ethyl hexanoate (C6). From these observations we conclude that molecules which are too short better interact with the receptor than those which are too long.

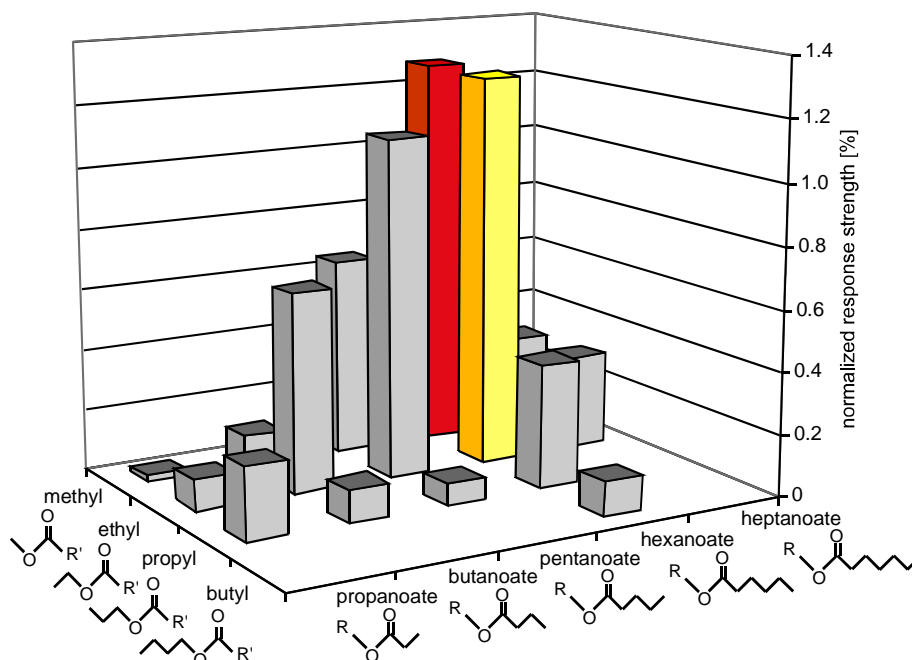


Figure 16 Ethyl and methyl hexanoate are the best ligands for ORNs expressing Or22a. The graph shows the ‘molecular landscape’ surrounding the best ligands identified out of the odor panel tested in this study. All odors shown are straight chain esters. The x-axis shows the carboxylic acid moieties ranging from C3 - propanoate to C7 - heptanoate. The y-axis shows the alcohol moieties ranging from CI - methyl to CIV - butyl. The z-axis indicates the mean normalized response to a concentration of 10^{-6} [vol/vol] ($n = 8$) of the respective odors. Color code as in previous figures.

In order to substantiate these observations further, in collaboration with Daniel Baum we employed an algorithm written by Daniel Baum (Baum, 2005) to align the three-dimensional structures of the esters depicted in Figure 16. The algorithm is based on the notion that multiple odors activating a given OR, although different in many respects, must share certain odotopes which are recognized by the receptor. Thus finding a substructure common to all activating odors of an OR will provide

hints to its binding site. Currently, application of the algorithm does not necessarily result in a single optimal alignment of the molecules included in the analysis to the reference molecule but can result in several equally rated alignments. Based on knowledge of the experimental data the user can choose the alignment that fits the experimental data best.

The algorithm required preselecting a reference molecule, in this case ethyl hexanoate. The result of this alignment confirmed the above described odotopes of Or22a. Figure 17A shows the alignment of 14 esters (methyl-, ethyl-, and propyl propionate, methyl-, ethyl-, and propyl butanoate, methyl-, ethyl-, and propyl pentanoate, methyl-, ethyl-, and propyl hexanoate, methyl- and ethyl heptanoate) with ethyl hexanoate as reference molecule. The presence of a carbon atom in the fifth position of the carboxylic acid moiety (5, black circle) could be shown to distinguish between activating and non-activating esters: all molecules with a carbon atom at this position elicited a response; those molecules without a carbon atom at this position did not elicit a response. However, there were two exceptions to this rule. The first exception was ethyl butanoate which does not have a carbon atom in this position yet elicited the fourth largest response. The second exception was propyl pentanoate for which no conformation with its fifth carboxylic acid carbon atom in the respective position could be found (Figure 17A).

Applying the algorithm to align the molecules belonging to the Or22a MRR (for the molecular structure of these molecules see Figure 10) resulted in the identification of a common substructure consisting of an oxygen atom (a) and three carbon atoms (1 to 3). Additionally, there were two positions where a large number of molecules had an additional oxygen atom (oxygen b and c). Oxygen 'c' was found in all acetate esters. The acetate ester group was aligned to the common substructure opposite to the non-acetate ester group. Non-acetate esters had their second oxygen atom in position 'b'. Oxygen 'c' was opposite to oxygen 'b' and both were accessible for possible binding sites. Thus we reasoned that these oxygen atoms could be bound via hydrogen bonds by the same binding site of Or22a, explaining low EC50 of for instance 2-methyl-butyl acetate. Looking at the aligned molecules from above showed that this side is almost entirely free thus putatively providing positions for hydrogen bonds with oxygen atom 'a' and hydrophobic forces acting on the carbon chain

(carbon atoms 1 to 3). A number of molecules could not be fitted by the algorithm to the substructure shown in Figure 17B. These were 2-butanone, 2-hexanone, 3-hexanone, pentanal, 2,3-butanedione, hexanal, β -butyrolactone, and ethyl acetate. It was however possible to manually align these molecules with the substructure showing that there are conformations which would allow those molecules to fit to the common identified substructure. For some odors we were only able to align the R-isomers with the common substructure (ethyl-2-methyl butanoate, 1-octen-3-ol, 3-octanol, 3-hydroxy-2-butanone, and 4-methylcyclohexanol, where alignment of the Z enantiomer was possible but not of the E enantiomer). Stimulating Or22a with pure isomers of the respective odors could reveal whether the receptor is indeed selective for the R-isomers (or Z-enantiomer) of those odors. The results show that all odor molecules found to activate Or22a have a putative common motif which could interact with the same receptor binding site.

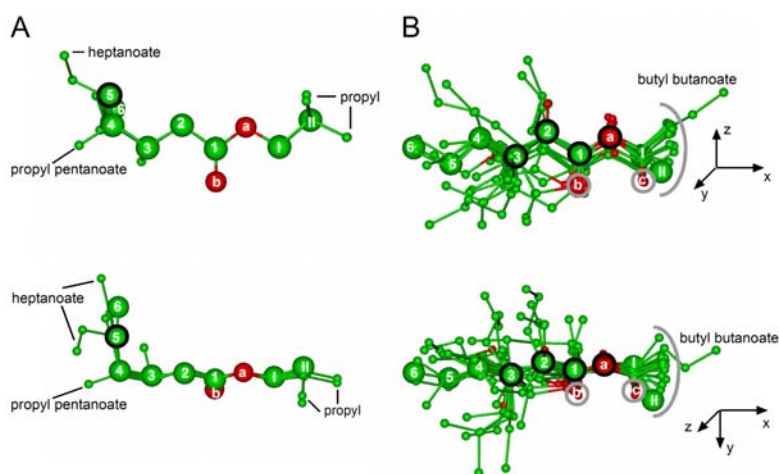


Figure 17 3D superposition of odors activating Or22a. The balls indicate atoms (red = oxygen, green = carbon, [hydrogen was omitted for clarity]), the sticks indicate atomic bonds. The enlarged balls emphasize ethyl hexanoate, the reference molecule for the superposition of the other molecules. The Arabic numbers label the carbon atoms of the hexanoate moiety, the roman numbers label the carbon atoms of the alcohol moiety and the letters label the oxygen atoms of the ester group. **A** Superposition of 14 esters (methyl-, ethyl- and propyl propanoate, methyl-, ethyl- and propyl butanoate, methyl-, ethyl- and propyl pentanoate, methyl-, ethyl- and propyl hexanoate, methyl- and ethyl heptanoate). Note how the propyl moieties and the heptanoate moieties extend beyond the 3D structure of ethyl hexanoate which represents the putative most potent ligand. The absence or presence of a carbon atom at the fifth position of the carboxylic acid moiety (5, black circle) was found to largely explain the distinction between activating and non-activating esters. **B** Superposition of the molecules belonging to the Or22a MRR. The atoms marked with black circles show the substructure present in activating odors. The oxygen atoms marked with grey circles are only present in a subset of odors. The grey half circle delineates the boundary of the ethyl group beyond which only butyl butanoate extended. Note how the upper part of the superposition is free for putative binding to the receptor.

In conclusion we determined ethyl and methyl hexanoate, which had been previously identified as natural odors for *D. melanogaster* (Stensmyr et al., 2003b) as most potent ligands for ORNs expressing Or22a. Furthermore, we were able to identify some of the odotopes which make ethyl and methyl hexanoate primary agonists for ORNs expressing Or22a.